Journal of Applied Polymer Science

Influence of an oligomer polyol and monomers on the structure and properties of core–shell polyurethane–poly(*n*-butyl acrylate-*co*-styrene) hybrid emulsions

Tao Wu, Xiulan Xin, Hongqin Liu, Baocai Xu, Xiaoyan Yu
School of Food and Chemical Engineering, Beijing Technology and Business University, Beijing 100048, China
Correspondence to: X. Xin (E-mail: xinxl2007@126.com)

ABSTRACT: The free-radical polymerization of alkenyl-terminated polyurethane dispersions with styrene and *n*-butyl acrylate was performed to obtain a series of stable polyurethane–poly(*n*-butyl acrylate-*co*-styrene) (PUA) hybrid emulsions. The core–shell structure of the emulsions was observed by transmission electron microscopy, and the microstructure was studied by ^{1}H-NMR and Fourier transform infrared spectroscopy. The effects of the poly(propylene glycol)s (number-average molecular weights = 1000, 1500, and 2000 Da) and the mass ratios of polyurethane to poly(*n*-butyl acrylate-*co*-styrene) (PBS; 50/50, 40/60, 30/70, 20/80, and 10/90) on the structure, morphology, and properties of the PUAs were investigated. The average particle size and water absorption values of the PUAs increased with increasing of PBS content. However, the surface tension decreased from 34.61 to 30.29 mN/m. PUA-2, with a bimodal distribution, showed Newtonian liquid behaviors, and PUA-3 showed a great thermal stability, fast drying characteristics, and excellent adhesion to packaging films. © 2016 Wiley Periodicals, Inc. J. Appl. Polym. Sci. **2016**, *133*, 43763.

KEYWORDS: emulsion polymerization; monomers; oligomers and telechelics; polyurethanes

Received 14 October 2015; accepted 8 April 2016
DOI: 10.1002/app.43763

INTRODUCTION

Polyols acting as the soft segment of polyurethane (PU) play an important role in the emulsion properties, such as the waterproofing, adhesion, and malleability.[1] In general, it is imperative that an oligomer polyol molecule contain at least two hydroxyl groups or other hydrogen donors (—NH_2, —COOH, —SH, etc.).[2,3] In recent years, oligomer polyols modified from castor oil, rapeseed oil, or soybean oil have been used to improve the PU properties, including the antiabrasion properties, heat resistance, and mechanical behavior.[4–6] Common reagents for the preparation of urethane polymers, apart from polyols, include diisocyanates, hydrophilic chain extenders, and end-capping reagents or subsequent chain extenders. As for poly(ether glycol), it is more flexible and foldable than poly(ester glycol), which is frequently considered as the ideal polyol to be widely used in coatings, inks, adhesives, leather, and so on.[7–11] With some shape-memory materials taken as examples, large-molecular-weight poly(ether glycol) is an important component for effecting the memory capacity of productions because of the good crystallinity of this kind of oligomer polyol.[12,13]

Polyurethane–poly(*n*-butyl acrylate-*co*-styrene) (PUA) hybrids exhibit excellent properties because the performance of PU and polyacrylate (PA) components is complementary through crosslinking and compounding. PUs possess excellent flexibility, adhesion, film formation, and abrasion resistance.[14–16] However, their water resistance, hardness, and weatherability are inferior to that of PA.[17,18] Currently, a large number of articles and reports have mentioned the preparation of PUA hybrid emulsions. Among all kinds of strategies, physical blending is one of the simplest approaches for integrating the PU and PA components, but it has a poor compatibility compared to emulsion copolymerization, chemical crosslinking, and grafting.[19–21] For instance, Athawale and Kulkarni[22] made a comparison between the core–shell structure and interpenetrating network structure of PUA hybrids via emulsion copolymerization techniques. Their works verified that the core–shell hybrids had better mechanical behavior than interpenetrating network hybrids because of the good compatibility between PU and PA monomers.

Although the intrinsic characteristics, such as the ionic group content, hard-segment/soft-segment molar ratio, physicochemical characteristics, and other external factors of PUA hybrid emulsions as the binder of coatings or water-based inks have been reported,[23–25] there have been few systematic studies exploring the relationship among the structure, rheological behavior, and printing adaptability via changes in the molecular weight of the oligomer polyol and the content of poly(*n*-butyl acrylate-*co*-styrene) (PBS). In this study, a series of PU

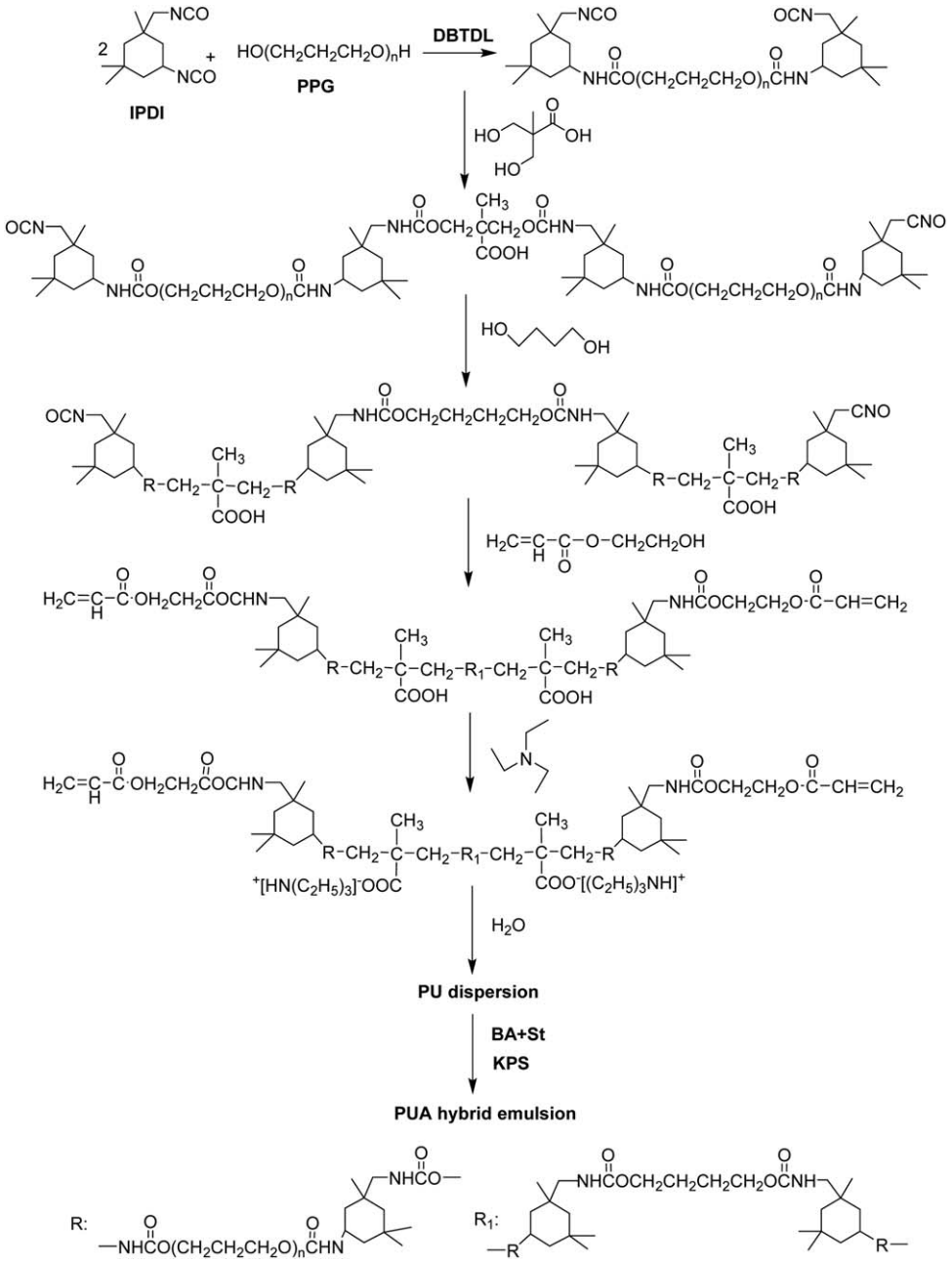

Scheme 1. Flow diagram of the PU dispersions and PUA hybrid emulsions.

dispersions were synthesized with poly(propylene glycol) [PPG; number-average molecular weights (M_ns) = 1000, 1500, and 2000 Da], and the samples were recorded from PU-1 to PU-3, respectively. PUAs were prepared from a PU dispersion and PBS monomers via semicontinuous seed emulsion polymerization, in which the mass ratio of PU and acrylics was from 50/50 to 10/90. The structure, morphology, and basic properties of the emulsions were investigated.

EXPERIMENTAL

Materials

Isophorone diisocyanate (IPDI; 99%) and *N*-methyl-2-pyrrolidone were purchased from Shangdong Xiya Chemical Industry Co., Ltd. PPG (M_ns = 1000 and 2000 Da) from Shanghai Aladdin Industrial Corp. were dried in a vacuum-drying oven at 110 °C for 3 h. Dibutyltin didodecylate (DBTDL) and sodium bicarbonate ($NaHCO_3$) received from Sinopharm Chemical Regent Co., Ltd. Dimethylol propionic acid (DMPA; 99%) was supplied by Acros Organics Co., Ltd. (New Jersey). Acetone (99.5%), 1,4-butanediol (BDO; 99%), hydroxyethyl acrylate (HEA; 97%), and triethyl amine (99%) were supplied by Tianjin Guangfu Fine Chemical Research Institute. Sodium dodecyl sulfate (SDS) and polyoxyethylene octylphenol ether (OP-10) were received from Tianjin Chemical Reagent Factory. Potassium persulfate (KPS; 98%) was recrystallized before it was used. Styrene (St; 98%) and *n*-butyl acrylate (*n*-BA; 98%) were distilled to

Table I. Recipes of the PU Dispersions.

	Reagent (molar ratio × 10^2)							
	IPDI	PPG (M_n = 1000 Da)	PPG (M_n = 2000 Da)	DMPA	BDO	HEA	Ionic group content (wt %)	Soft-segment content (wt %)
PU-1	5.00	1.25	—	1.00	0.95	1.00	5.00	46.30
PU-2	5.00	0.625	0.625	1.25	0.65	1.00	5.00	56.35
PU-3	5.00	—	1.25	1.50	0.45	1.00	5.00	63.01

R is defined as the molar ratio of —CNO in IPDI to —OH in PPG, DMPA, BDO and HEA. (—CNO/—OH) = 1.2. The solid content of PUs was 30%.

remove the inhibitors. Deionized water was used throughout the study, and all of the materials were used without further purification. Poly(vinyl chloride) (PVC), polyamide (PA), poly (ethylene terephthalate) (PET), polyethylene (PE), and biaxially oriented polypropylene (BOPP) were purchased from the market.

Methods

Preparation of the Waterborne PU Dispersions. IPDI and PPG were charged into a 250-mL, four-necked glass reactor equipped with a mechanical stirrer, thermometer, reflux condenser, and nitrogen protection. The reaction was carried out at 55 °C. During stirring, DBTDL (0.3 wt % on the basis of the total PU weight) as a catalyst was added to the flask; then, the reaction mixture was stirred for 1 h at 80 °C to obtain an NCO-terminated prepolymer. Then, DMPA (dissolved in *N*-methyl-2-pyrrolidone) was added to this system until the residual NCO groups of the prepolymer reached the desired value measured by the standard dibutylamine back-titration method (ASTM D 1638). Subsequently, BDO and HEA were added to the system to react with the residual isocyano (—CNO), respectively, and the reaction mixture was diluted by appropriate acetone. Until the reaction temperature was down to 40 °C, triethyl amine (95 wt % of DMPA) was added to the reactor to neutralize the carboxyl of alkenyl-terminated prepolymer for 0.5 h. Ultimately, deionized water was added to the flask at about one drop per second with stirring at a rate of 1000 rpm to disperse the prepolymer for 30 min. Finally, an alkenyl-terminated polyurethane (ATPU) dispersion was obtained with translucent blue light. The flow diagram of the PU dispersion is shown in Scheme 1, and the main feed composition of the PU dispersion is listed in Table I.

Synthesis of the PUA Hybrid Emulsion. The pre-emulsion was prepared by the mixture of SDS, OP-10, $NaHCO_3$, and distilled water at room temperature. Then, St and the butyl acrylate (BA) monomers (mass ratio = 7:3) were slowly dropped into the reactor at about one drop per 5 s with stirring at a rate of 200 rpm.

The PUAs were synthesized from the ATPU dispersion with pre-emulsion via free-radical polymerization under N_2 protection. First, the 15 wt % pre-emulsion and KPS were added to the PU dispersion with mixing at 40 °C for 0.5 h. Then, the residual pre-emulsion and KPS were slowly dropped into the system at 80 °C for 4 h. After each component was thoroughly added, the whole reaction continued at 80 °C for another 2 h to obtain the final hybrid emulsion. The synthesis process of the PUAs is shown in Scheme 1. Each component for the PUAs is displayed in Table II.

Preparation of the PUA Hybrid Emulsion Films. Hybrid emulsions were placed into glass molds at room temperature for 7 days to dry naturally. Then, polymer films were transferred to a vacuum-drying oven at 40 °C for another 24 h. After the previous two steps, the films were stored in a desiccator for further study.

Characterization

Particle Size and Distribution. The particle size and polydispersity index (PDI) of the PUA hybrid emulsions were measured with a Malvern Zetasizer Nano-ZS instrument. The samples were diluted to 10–15 wt % with deionized water before the measurement. PDI was obtained from nonnegative least squares analysis and calculation. PDI was expressed mathematically as follows:

$$\mathrm{PDI} = \sigma^2 / Z_D^2$$

where σ is the standard deviation and Z_D is the average particle diameter.

^{1}H-NMR Spectral Analysis. The ^{1}H-NMR spectra of PU and PUA were characterized by a Bruker Fourier 300-MHz spectrometer with $CDCl_3$ as the solvent and tetramethylsilane (TMS) as the internal standard.

Fourier Transform Infrared (FTIR) Spectral Analysis. The IR spectra of the samples were recorded on a Nicolet 5700 instrument (Thermo Co.).

Transmission Electron Microscopy (TEM) Testing. The morphology of the polymer films were studied with a JEM-2100 transmission electron microscope at 200 kV. The samples were stained with a 2% phosphotungstic acid solution.

Rheological Behavior Testing. The surface tension of the emulsions was performed on a Dataphysics-DCAT11 with the Wilhemy plate method at 25 ± 0.1 °C, and the viscosity (η) of the emulsions was determined by a Haake MARS instrument (CC25 DIN Ti) at 25 °C.

Water Absorption Testing. A certain quality of polymer films (the origin weight was recorded as ω_1) was immersed in distilled water at room temperature for 24 h. Then, the residual water was wiped with filter paper, and the immediate weight (ω_2) of the films was measured. The water absorption was calculated according to the following formula:

Table II. Compositions of the PUA Hybrid Emulsions

Sample	PU dispersion (g)			Emulsifier (g)		KPS (g × 10)	Monomer (mmol/g)		Distilled water (mmol/g)
	PU-1	PU-2	PU-3	SDS	OP-10		St	*n*-BA	
PUA-1	66.67			0.53	0.27	0.80	1.35	0.47	6.94
PUA-2		66.67		0.53	0.27	0.80	1.35	0.47	6.94
PUA-3			66.67	0.53	0.27	0.80	1.35	0.47	6.94
PUA-4			53.33	0.64	0.32	0.96	1.62	0.56	12.18
PUA-5			40.00	0.75	0.37	1.12	1.88	0.66	17.29
PUA-6			26.67	0.85	0.43	1.28	2.15	0.75	22.47
PUA-7			13.33	0.96	0.48	1.44	2.42	0.84	27.66

The total mass of the system was 100 g.

$$\text{Water absorption } (\%) = (\omega_2 - \omega_1)/\omega_1 \times 100\%$$

Drying Rate Testing. The drying rate of the emulsions was determined by the vacuum-drying oven at 50 °C. In 90 min, the samples were measured every 10 min; then, the measurement time intervals were 0.5, 1, 3, 6, and 10 h. The measurements were done until the weights of the samples were constant. The concrete calculating formula for the polymers is as follows:

$$Deh\,(\%) = \frac{E_1 - E_t}{E_1 \times (1-S)} \times 100\% \quad (t = 1, 2, 3 \ldots)$$

where *Deh* is the dehydration rate of the emulsion during the drying process (%), E_1 is the initial mass of the emulsion (g), E_t is the mass of the emulsion at time t (g), and S is the solid content of the emulsion (%)

Adhesion Testing. The adhesion of the samples on different packaging films (PVC, BOPP, PA, PE, and PET) were tested according to ASTM D 3359-09. A lattice pattern with 11 cuts in each direction was made in the emulsion film to the substrate; pressure-sensitive tape was applied over the lattice and then removed, and adhesion was evaluated by a comparison with descriptions and illustrations. We rated the adhesion in accordance with following scale, as illustrated in Table III.

Thermogravimetric Analysis (TGA). The thermal stability of the emulsion films was measured by a DTG-60AH instrument (Shimadzu, Japan). The samples with the same quality were placed in a small metal pot and heated from 0 to 600 °C under N_2 protection.

RESULTS AND DISCUSSION

Particle Size and Distribution

The particle size and distribution of the emulsions are depicted by Figure 1. There was no big difference in the particle sizes among all of the samples. The only change was that the particle size distribution increased with increasing PPG molecular weight and content in the polymer, whereas PUA-2 presented a bimodal distribution with peaks around 76 and 192 nm. This result was attributed to the fact that the hydroxyl activity of PPG ($M_n = 1000$ Da) was higher than that of PPG ($M_n = 2000$ Da) for the short carbon chain.[26] In addition, the average particle sizes and PDIs of the emulsions were determined as the change of the PPG content and molecular weight (Table IV). An increase in PDI was observed with increasing molecular weight of PPG. This was attributed to the repulsive forces between the ionic moieties of the PU dispersion.

From PUA-3 to PUA-7, the average particle size increased with increasing PBS monomer, and it remained around 86–139 nm (Table IV). When PBS was introduced into the copolymer, the ionic moieties of the PU dispersion started to decrease; this might have decomposed the original micellar structure to form large particles via free-radical polymerization.[27] Furthermore, when the mass ratio of PU/PBS was less than 30/70, a small amount of coagulum may have been triggered because the polymerization of the residual monomers may have occurred outside of the PU polymer. Therefore, it was significant to control the dosage of the PBS monomers to gain stable and small-particle-size hybrid emulsions.

Table III. Classification of the Adhesion Test Results

Classification	Area removed (%)
5B	The edges of the cuts were completely smooth; none of the squares of the lattice were detached.
4B	Small flakes of the film were detached at intersections; less than 5% of the area was affected.
3B	Small flakes of the film were detached at intersections of cuts; the affected area was 5–15% of the lattice.
2B	The film flaked along the edges and on parts of the squares; the affected area was 15–35% of the lattice.
1B	The film flaked along the edges of cuts in large ribbons, and whole squares had detached. The affected area was 35–65% of the lattice.
0B	Flaking and detachment were worse in comparison with 1B.

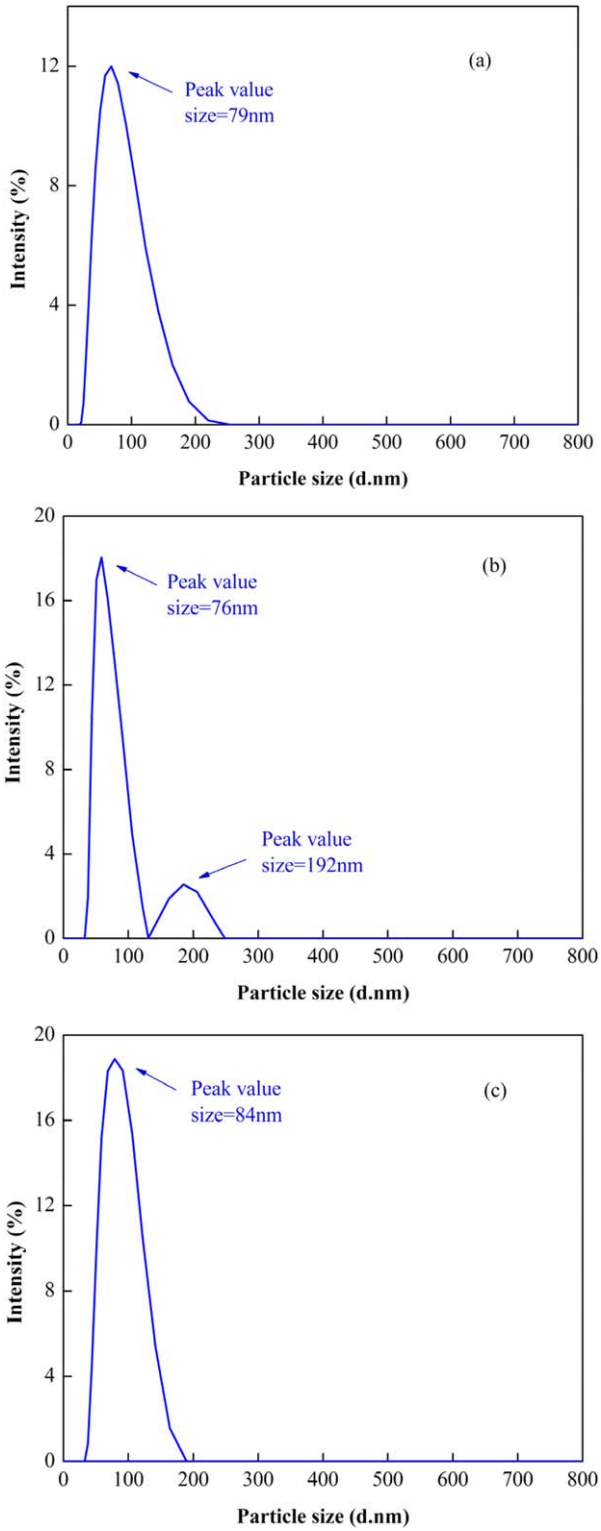

Figure 1. Particle size and distribution of hybrid emulsions: (a) PUA-1, (b) PUA-2, and (c) PUA-3. [Color figure can be viewed in the online issue, which is available at wileyonlinelibrary.com.]

Structure of the Polymers

^{1}H-NMR Spectral Analysis. PU-3 and PUA-3 were characterized by ^{1}H-NMR spectroscopy. As shown in Figure 2, there was a similar chemical shift between PU-3 and PUA-3 on account of the same position of hydrogen protons. In Figure 2(a), the proton of the —C—CH_2—O— units was observed in the range δ = 3.38–3.70 ppm (c, l, n).[28] The weak peak at 4.08 ppm (e) may have indicated the reaction with the units of —CH_2—NH—COO— in the hard segment of PU. In addition, the active methyl (—CH_3) and methylene (—CH_2—) protons of the diisocyanate moieties were observed in the range 0.87–1.68 ppm (g, j, k) for the spin–spin coupling–splitting of protons. As compared to Figure 2(a), it was obvious that PUA-3 had a similar structure in terms of the PU segment shown in Figure 2(b). The peaks of δ at 6.68–7.08 ppm (v, w, x) belonged to the aromatic protons; this indicated the introduction of the St monomer in the course of emulsion polymerization, which was a remarkable difference between the two samples. Apart from the disappearance of peaks in the range 3.05–3.07 ppm, this verified that the terminal double bonds of PU reacted completely with the monomers.

FTIR Spectral Analysis. The chemical structure of the PUAs were analyzed by FTIR spectroscopy (shown in Figure 3). As shown from the spectra, the stretching frequency of the N—H group was observed in the range 3334–3343 cm^{-1}. The stretching vibrations of ether bonds (C—O—C) appeared from 2967 to 2872 cm^{-1}. This result demonstrated the existence of the hydrogen-bond interactions between the PU chain and the reactive hydrogen of NHC═O.[29] The characteristic bands around 2930, 1727, and 1607 cm^{-1} confirmed the methylene and methyl groups (CH_2 and CH_3) of PPG, carbonyl group (C═O) of urethane–urea, and cyano groups (C—N) of carbamido, respectively. The stretching vibration peak of —CNO around 2360 cm^{-1} did not appear in Figure 3; this indicated that the residual —CNO was thoroughly consumed during the process of the curing of the emulsion.

According to analysis of ^{1}H-NMR and FTIR spectroscopy, we proved that the backbone of PU-3 and PUAs was formed.

TEM Testing. The morphology of the emulsions (from PUA-1 to PUA-3) is shown in Figure 4. A clear core-phase and shell-phase structures of the emulsions was observed, in which the light and dark regions of the particles corresponded to PU and PA polymers, respectively. Moreover, the observed particle size of the emulsions was consistent with the results obtained in Figure 1. We discovered that the particle size of PUA-1 was nearly the same as that of the PUA-3 when a small amount of

Table IV. Average Particle Sizes and PDIs of the PUA Hybrid Emulsions

Sample	PU/PA	Average particle size (nm)	PDI
PUA-1	50/50	90	0.225
PUA-2	50/50	108	0.509
PUA-3	50/50	86	0.072
PUA-4	40/60	87	0.116
PUA-5	30/70	92	0.181
PUA-6	20/80	119	0.178
PUA-7	10/90	139	0.551

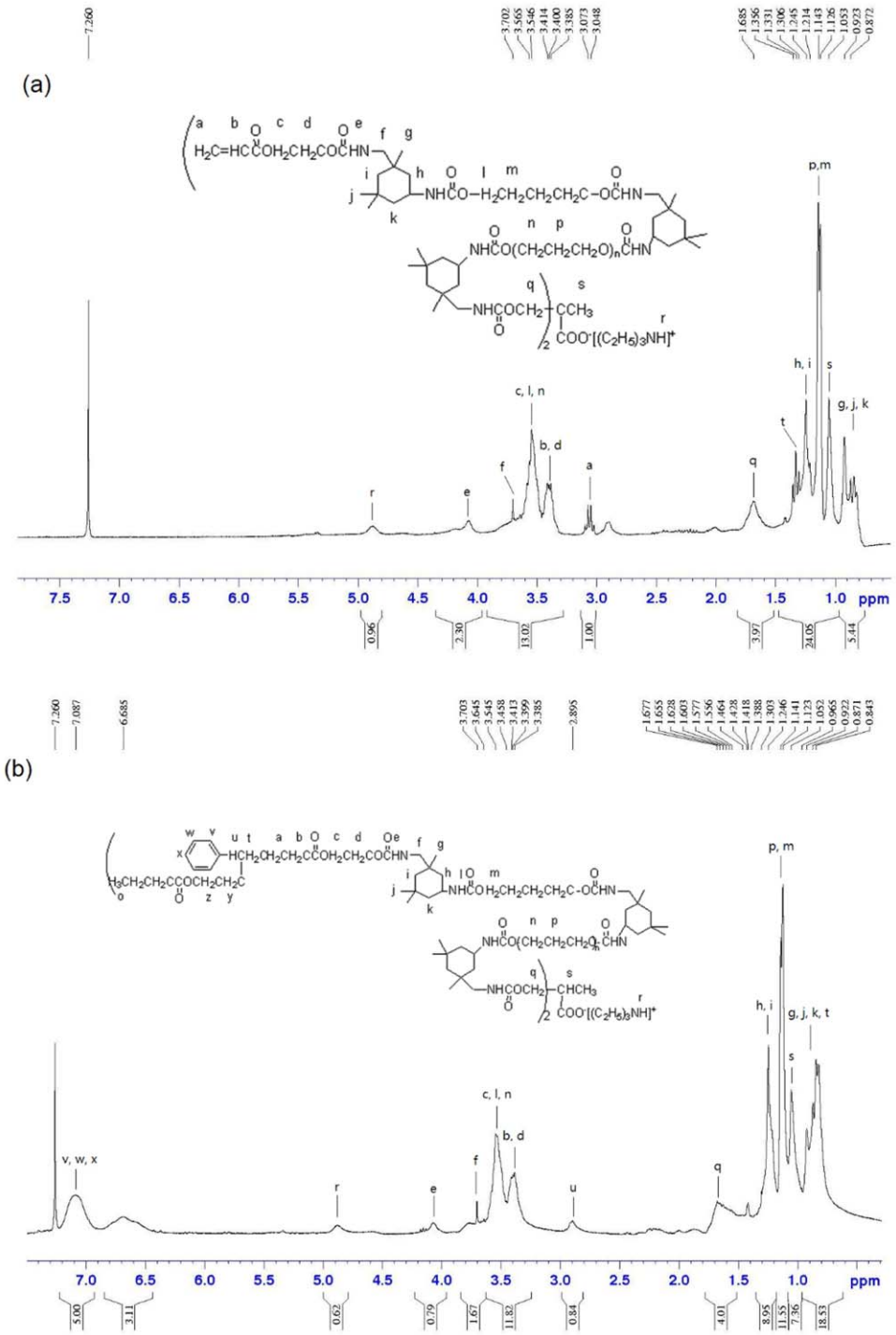

Figure 2. [1]H-NMR spectrum of the (a) PU-3 dispersion and (b) PUA-3 hybrid emulsion. [Color figure can be viewed in the online issue, which is available at wileyonlinelibrary.com.]

n-BA and St monomers were incorporated. This indicated that PPG with the single molecular weight was conducive for forming the hybrid emulsion with a unimodal particle distribution. However, PUA-2 with different lengths of PU chains resulted in a bimodal particle distribution and a small number of larger particles. Thus, the molecular weight of the oligomer diol that reacted as the composition of the PU dispersion influenced the particle size of the final hybrid emulsion.

Properties of the PUAs

Rheological Behavior Testing. Figure 5 describes the relationship among the shear force (τ), η, and shear rate (γ) of the emulsions. As shown in Figure 5(a), τs of PUA-1 and PUA-3 increased nonlinearly with increasing γ. This result revealed that the emulsions exhibited the pseudoplastic liquid behaviors, whereas PUA-2 showed Newtonian rheological behavior under the same conditions. As shown in Figure 5(b), all of the

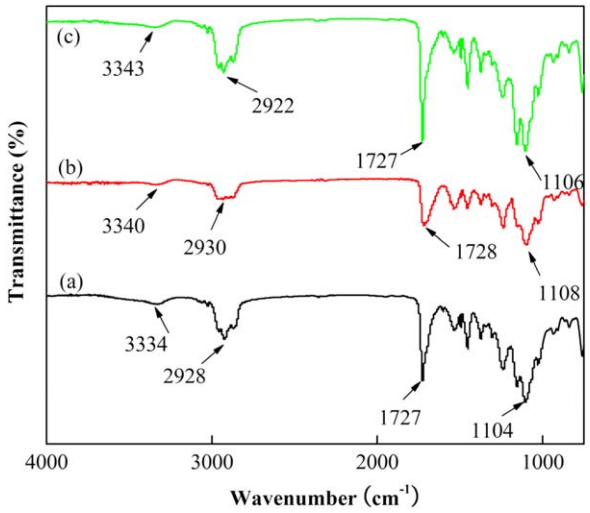

Figure 3. FTIR spectra of the films of the PUAs (PUA-1, PUA-2, and PUA-3). [Color figure can be viewed in the online issue, which is available at wileyonlinelibrary.com.]

emulsion samples exhibited shear-thinning behaviors in the whole stage except PUA-2 approached a constant value above a γ of about 400 s^{-1}. This result corresponded to the rheological behaviors of the emulsions; this indicated that PUA-2 was a Newtonian liquid, and there was no significant interaction among the suspended particles. Moreover, the shear η of emulsions decreased with increasing particle size and PUA-2 exhibited a low shear η in the initial stage. Because the small particles had a lower porosity and a higher packing density in the emulsion center than the large particles, this caused a high shear η and pseudoplastic liquid behavior in PUA-1 and PUA-3. However, conversely, PUA-2 exhibited a bimodal distribution, and a small amount of large particles was distributed in the emulsion; this may have been the reason for the low η and Newtonian liquid.

As shown in Figure 6, the surface tension of the PUAs was observed by the Wilhemy plate method. From PUA-1 to PUA-3, the surface tension of PUA-2 was bigger than the others for the high polarity of the emulsion. However, when the mass ratio of PU/PBS decreased from 50/50 to 10/90, the surface tension of

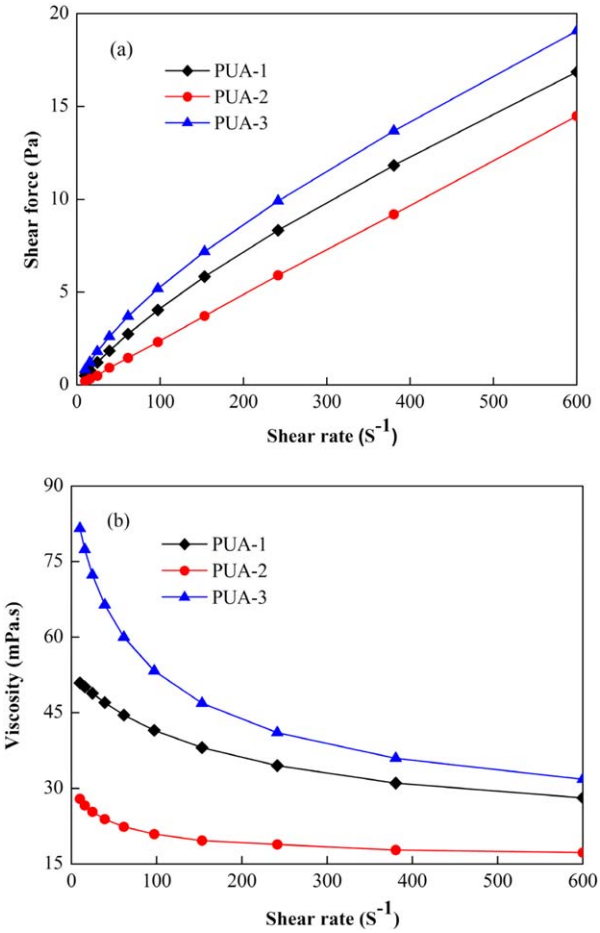

Figure 5. τ and η values of the PUAs: (a) τ–γ and (b) η–γ. [Color figure can be viewed in the online issue, which is available at wileyonlinelibrary.com.]

emulsions decreased from 34.61 to 30.29 mN/m. This result was attributed to the fact that the electronic cloud density around the PU chains was higher than that around the PBS monomer, especially in soft segments.[30,31]

Water Absorption Testing. The water absorption rate of the emulsion films is shown in Figure 7. When the mass ratio of

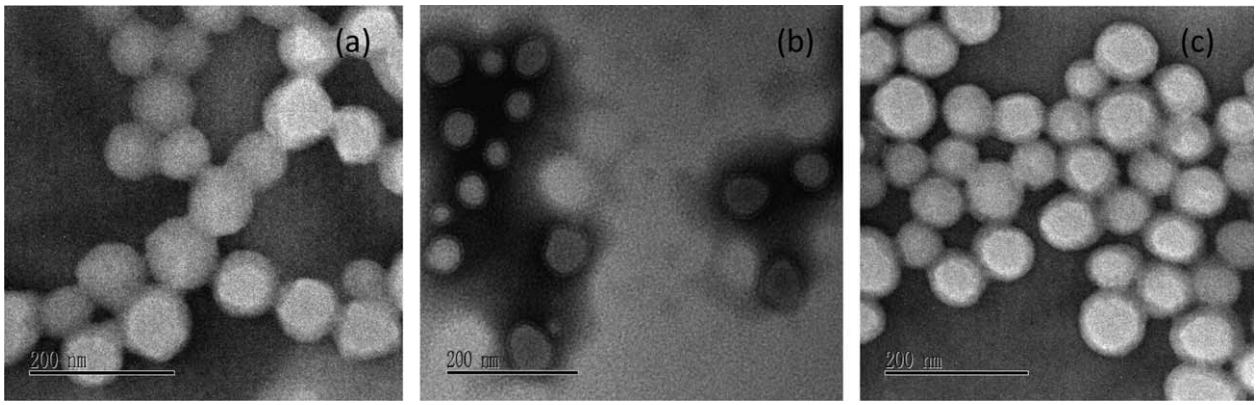

Figure 4. TEM images of the PUAs: (a) PUA-1, (b) PUA-2, and (c) PUA-3.

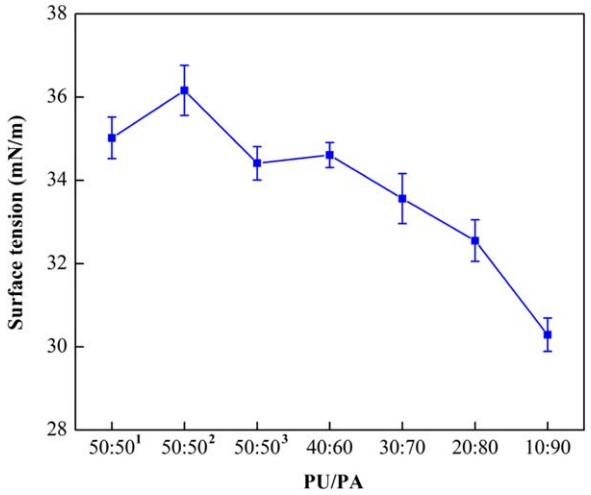

Figure 6. Values of the surface tension with various ratios of PU to PBS (PU/PBS = 50:50^n corresponding to PUA-*n*, *n* = 1, 2, and 3). [Color figure can be viewed in the online issue, which is available at wileyonlinelibrary.com.]

PU/PBS was 50:50, the water absorption of PUA-3 was lower than that of the other two samples. This result indicates that PU with large-molecular-weight PPG had better water resistance than the ones with small molecular weights. The emulsion film with the large-molecular-weight oligomer polyol was conducive to the formation of a compact layer during the curing course, so water hardly permeated this obstacle to the inside. At a mass ratio of PU/PBS from 50:50 to 10:90, water absorption increased with increasing content of PBS. For all of the samples, we found that PUA-3 had the smallest water absorption rate; this illustrated that a large molecular weight may be a way to improve the water resistance of emulsion films.

Drying Rate Testing. In general, the drying rate is a key factor in water-based ink printing on packaging films; this effects the efficiency and quality production.[32] As for the drying mechanism of emulsions on packaging films, the curing process can

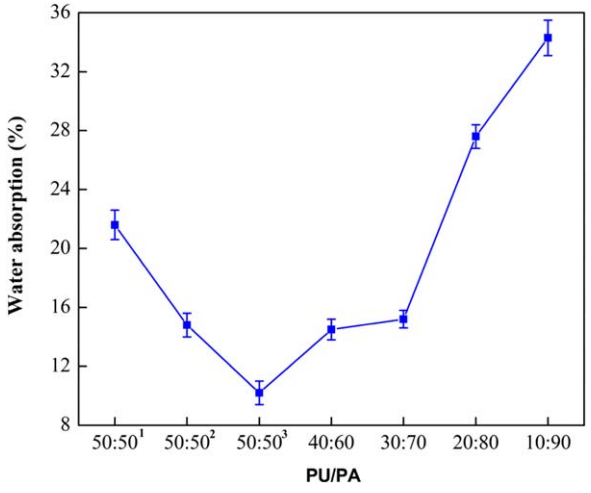

Figure 7. Water absorption of the PUAs (PU/PBS = 50:50^n corresponding to PUA-*n*, *n* = 1, 2, and 3). [Color figure can be viewed in the online issue, which is available at wileyonlinelibrary.com.]

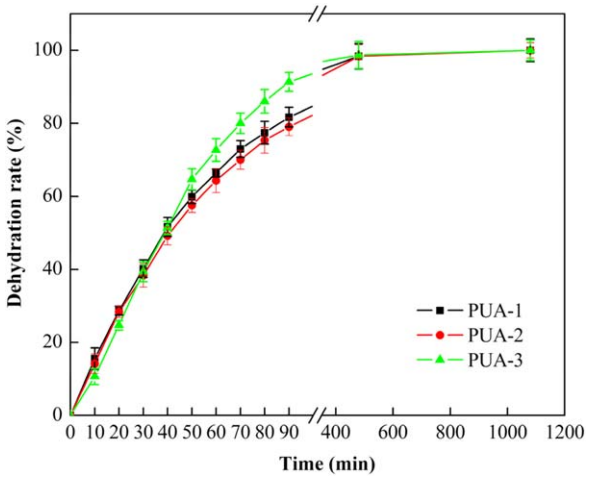

Figure 8. Dehydration rate of the PUA-1, PUA-2, and PUA-3 hybrid emulsions over time. [Color figure can be viewed in the online issue, which is available at wileyonlinelibrary.com.]

be divided into three steps: the first stage is the volatilization of little solvent and free water. Then, the second stage involves partial bound water, which evaporates from the inside to the surface of the emulsion through the capillary channel and the membrane permeability of the particles after free water loss. Finally, the polymer molecules start to close on each other gradually to form multilayer films, and the residual bound water can only penetrate these films to reach the surface until the emulsion is completely dry (third stage).

The changes in the water loss of PUAs over time are shown in Figure 8. The water loss of the samples was nearly the same at the initial stage (ca. 5 wt % water loss). Compared to the PUA-1 and PUA-2, PUA-3 presented a faster dehydration rate, and the water loss nearly approached 90 wt % before 90 min. However, to remove the residual moisture of the emulsions, another 6–7 h was needed according to Figure 8. This result was in accordance with the drying mechanism of the emulsions, and the drying time of PUA-3 was short in the second and third stages; this was attributed to the small particle sizes and low surface tension. In addition, the core–shell structure of the emulsion may also have played a supplementary role because the glass-transition temperature of the core was higher than that of the shell; this accelerated the curing of the emulsion.

Table V. Adhesion of the PUAs to the Packaging Films

	Adhesion				
Sample	PVC	BOPP	PA	PET	PE
PUA-1	5B	3B	5B	5B	5B
PUA-2	5B	2B	5B	5B	5B
PUA-3	5B	1B	5B	5B	5B
PUA-4	5B	0B	5B	4B	5B
PUA-5	5B	0B	5B	3B	5B
PUA-6	5B	0B	5B	3B	5B
PUA-7	4B	0B	5B	3B	5B

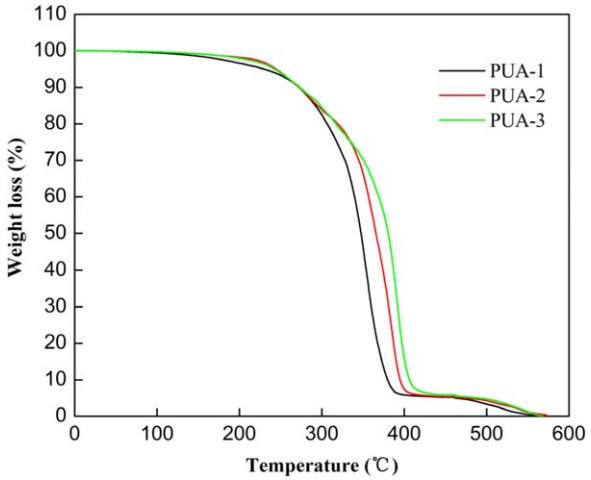

Figure 9. TGA curves of PUA-1, PUA-2, and PUA-3. [Color figure can be viewed in the online issue, which is available at wileyonlinelibrary.com.]

Therefore, an emulsion with a core–shell structure, small particle size, and low surface tension shortened the drying time.

Adhesion Testing. The adhesion of the emulsions on the packaging films (PVC, BOPP, PA, PE, and PET) was measured by a cross-cut tape test, and the result is shown in Table V. We observed that all of the emulsions on the BOPP film exhibited poor adhesion among the five kinds of substrates. This result was primarily ascribed to the nonpolar and low-surface free energy of the BOPP film, and the emulsion hardly showed good adhesion on the surface of this film. This would be an obstacle to ink printing adaptability. Therefore, there are some specific surface treatments needed for the BOPP film before it is used.[33] As for PUA-3 to PUA-7, the adhesion of the emulsions on the PA and PE film was excellent for the high surface free energy of these films. However, the adhesion of the emulsions on the PVC, BOPP, and PET films decreased at different degrees with increasing St and BA content because of the weak polarity of PBS. This result indicated that PUA-3 was the optimum conditions of the emulsion adhesion on the packaging films.

TGA. The thermal stability of the samples (from PUA-1 to PUA-3) was evaluated in the range of 0–600 °C, and the result is shown in Figure 9. The decomposition of the emulsion film was divided into three stages. In the first stage, the terminal PA of the emulsion film started to decompose in the range 0–200 °C because of the relatively low thermal stability. Then, most of the hard and soft segments of PU were decomposed, and the weight loss reached a maximum that approached to 77–85% in the range 300–411 °C.[34] Finally, a small numbers of carbon chains and residual impurities were decomposed to a minimum when the temperature was 600 °C. As shown in Figure 9, all samples had great thermal stability in the first stage, but PUA-3 exhibited better thermal stability than PUA-1 and PUA-2 when the temperature was over 273 °C because PUA-3 with large-molecular-weight PPG enhanced the chemical bond and entanglement among the molecular chains. These results show that the large-molecular-weight oligomer polyol was conducive to improving the thermal stability of the emulsion films.

CONCLUSIONS

PU–acrylate hybrid emulsions were successfully synthesized by ATPU dispersions with St and *n*-BA and characterized by FTIR spectroscopy and ^{1}H-NMR. We also confirmed the existence of the core–shell structure of the PUA hybrid emulsion via the observation of the TEM images. The particle size distribution of the emulsions was effected by the chain length of PPG and PUA-2 with a bimodal distribution exhibited Newtonian liquid behavior. Furthermore, the average particle size decreased with increasing PBS monomers. The drying rate indicated that an emulsion with a small particle size and core–shell structure could shorten the drying time at 50 °C. The adhesion of the emulsions on the packaging films was mainly determined by the surface free energy of the substrate. The thermal stability of the PUAs was enhanced via the increase in the molecular weight of the emulsions. In summary, the core–shell PUA hybrid emulsion incorporated with the large-molecular-weight oligomer polyol might be of interest with respect to potential water-based ink applications.

ACKNOWLEDGMENTS

This work is supported by the National Nature Science and Foundation of China (21376008) and the Young Teachers' Scientific Research Foundation of Beijing Technology & Business University (QNJJ2015-13).

REFERENCES

1. Howard, G. T. *Int. Biodeter. Biodegrad.* **2002**, *49*, 245.
2. Chang, W. H.; Scriven, R. L.; Peffer, J. R.; Porter, S., Jr. *Ind. Eng. Chem. Prod. Res. Dev.* **1973**, *12*, 282.
3. Guan, J.; Song, Y. H.; Lin, Y.; Yin, X. Z.; Zuo, M.; Zhao, Y. H.; Tao, X. L.; Zheng, Q. J. *Ind. Eng. Chem. Res.* **2011**, *50*, 6517.
4. Lu, Y.; Larock, R. C. *Biomacromolecules* **2007**, *8*, 3109.
5. Gurunathan, T.; Mohanty, S.; Nayak, S. K. *J. Mater. Sci.* **2014**, *49*, 8017.
6. Philipp, C.; Eschig, S. *Prog. Org. Coat.* **2012**, *74*, 706.
7. Yu, F.; Saha, P.; Suh, P. W.; Suh, P. W.; Kim, J. K. *J. Appl. Polym. Sci.* **2015**, *132*, DOI: 10.1002/app.41410.
8. Dai, X. H.; Xu, J.; Guo, X. L. *Macromolecules* **2004**, *37*, 5651.
9. Lee, S. W.; Lee, Y. H.; Park, H.; Kim, H. D. *Macromol. Res.* **2013**, *21*, 711.
10. Ou, J. H.; Yang, Y.; Gan, J. Q.; Ha, C. Y.; Zhang, M. *J. Appl. Polym. Sci.* **2014**, *131*, DOI: 10.1002/app.40078.
11. Wang, X.; Hu, Y.; Song, L.; Xing, W. Y.; Lu, H. D.; Lv, P.; Jie, G. X. *J. Polym. Res.* **2011**, *18*, 722.
12. Lee, S. K.; Yoon, S. H.; Chung, I.; Hartwig, A.; Kim, B. K. *J. Polym. Sci. Part A: Polym. Chem.* **2011**, *49*, 638.
13. Kalita, H.; Karak, N. *Polym. Eng. Sci.* **2012**, *52*, 2457.
14. Jena, K. K.; Chattopadhyay, D. K.; Raju, K. *Eur. Polym. J.* **2007**, *43*, 1830.
15. Shin, M. S.; Lee, Y. H.; Rahman, M. M.; Kim, H. D. *Polymer.* **2013**, *54*, 4878.

16. Lopez, A.; Degrandi-Contraires, E.; Canetta, E.; Creton, C.; Keddie, J. L.; Asua, J. M. *Langmuir* **2011**, *27*, 3884.
17. Li, M.; Daniels, E. S.; Dimonie, V.; Sudol, E. D.; El-Asser, M. S. *Macromolecules* **2005**, *38*, 4188.
18. Shi, Y.; Wu, Y.; Zhu, Z. *J. Appl. Polym. Sci.* **2003**, *88*, 473.
19. Brown, R. A.; Coogan, R. G.; Fortier, D. G.; Reeve, M. S.; Rega, J. D. *Prog. Org. Coat.* **2005**, *52*, 79.
20. Mignard, N.; Okhay, N.; Jegat, C.; Taha, M. *J. Polym. Res.* **2013**, *20*, 1.
21. Peruzzo, P. J.; Anbinder, P. S.; Pardini, O. R.; Vega, J.; Costa, C. A.; Galembeck, F.; Amalvy, J. I. *Prog. Org. Coat.* **2011**, *72*, 432.
22. Athawale, V. D.; Kulkarni, M. A. *Pigment Resin Technol.* **2010**, *39*, 145.
23. Zhang, J. F.; Li, X. F.; Shi, X. H.; Hua, M.; Zhou, X. P.; Wang, X. Q. *Prog. Nat. Sci.* **2012**, *22*, 76.
24. Luo, X. M.; Zhang, P.; Ren, J.; Liu, R.; Feng, J. Y.; Ge, B. H. *J. Appl. Polym. Sci.* **2015**, *132*, 2.
25. El-Molla, M. M. *Dyes Pigments* **2007**, *74*, 374.
26. Asua, J. M. *Prog. Polym. Sci.* **2002**, *27*, 1289.
27. Zubitur, M.; Asua, J. M. *Polymer.* **2001**, *42*, 5983.
28. Wang, Y. Y.; Qiu, F. X.; Xu, B. B.; Xu, J. C.; Jiang, Y.; Yang, D. Y.; Li, P. L. *Prog. Org. Coat.* **2013**, *76*, 880.
29. Lee, B. S.; Chun, B. C.; Chung, Y. C.; Sul, K. I.; Cho, J. W. *Macromolecules* **2001**, *34*, 6435.
30. Asif, A.; Huang, C. Y.; Shi, W. F. *Colloid Polym. Sci.* **2004**, *2*, 204.
31. Hirose, M.; Zhou, J. H.; Nagai, K. *Prog. Org. Coat.* **2000**, *38*, 30.
32. Vandam, D. B.; Kuerten, J. G. M. *Langmuir* **2008**, *2*, 582.
33. Bichler, C. H.; Langowski, H. C.; Moosheimer, U.; Seifert, B. *J. Adhes. Sci. Technol.* **1997**, *11*, 241.
34. Ahmed, A.; Sarkar, P.; Ahmad, I.; Das, N.; Bhowmick, A. K. *J. Ind. Eng. Chem. Res.* **2015**, *54*, 52.